Segmentation and Mesh Generation for Patient-Specific Flow Modelling in Carotid Arteries

Igor Sazonov[1]
i.sazonov@swansea.ac.uk
Xianghua Xie[2]
x.xie@swansea.ac.uk
Si Yong Yeo[1]
genyeoius@gmail.com
Rhodri Bevan[1]
r.bevan@swansea.ac.uk
Raoul van Loon[1]
r.vanloon@swansea.ac.uk
Perumal Nithiarasu[1]
p.nithiarasu@swansea.ac.uk

[1] College of Engineering
Swansea University
Swansea, SA2 8PP, UK

[2] Department of Computer Science
Swansea University
Swansea, SA2 8PP, UK

Abstract

Segmentation and mesh generation are two important stages in patient-specific computational modelling. In this paper, we present our approach to these two problems in modelling blood flow haemodynamics in human carotid arteries in order to improve the understanding of the impact of flow dynamics to carotid disease formation and progression. The segmentation of carotid arteries in CT scans is carried out using a deformable model based on a geometrical potential force that is derived from generalising image gradient vector interactions across the image domain. It is shown to be robust towards image noise interference, weak edge, and arbitrary initialisations. The mesh generation involves surface meshing and volume meshing. The surface meshes are computed from the implicit function obtained from the deformable modelling. The near-wall volumetric mesh is required in order to resolve the viscous boundary layer in flow studies. A flow study on severe stenosis is provided which involves segmenting the carotid geometries, generating valid surface and volume meshes, and a flow solver.

1 Introduction

It is known that vascular diseases such as stenosis and aneurysms are often associated with changes in blood flow patterns and the distribution of wall shear stress (WSS). It is however extremely complicated to measure those flow parameters *in vivo* at present time. Numerical modelling of the haemodynamics, based on the geometries obtained from 3D scans, can provide valuable insights which may help to development of efficient treatment methods. In

recent years, computational fluid dynamics (CFD) has been increasingly used for patient-specific modelling of blood flow in vascular structures, but so far there has been very limited applications of computational haemodynamics in clinical practice. This is largely due to the challenges involved in the design of an integrated framework which can robustly and accurately automate the computational modelling process, which includes image segmentation, mesh generation, and computational fluid dynamics simulation.

Segmentation and subsequent mesh generation have shown to be an intricate procedure and often application dependent. Due to lack of generic methods and robust automation, performing computational modelling on a large scale of data is particularly difficult. In this work, we adopt a generic segmentation algorithm to obtain the carotid geometries from CT scans and a mesh generation approach which attempts to minimise user interference. We demonstrate the proposed approach on analysing wall shear stress pattern in severe stenosis. The results from this preliminary study show that the proposed method is a promising approach to an integrated, generic and automated patient-specific computational modelling.

2 Image segmentation

The GPF method. Among many others, deformable modelling is a popular approach to image segmentation, e.g. [6, 10]. Conventional techniques suffer from weak edge, image noise and convergence issues. For instance, in [6] a constant pressure force is necessary in order to improve its capture range, resulting in monotonic expanding or shrinking of the mode that is problematic. In this work, we adopt the Geometric Potential Force (GPF) based deformable model [12] to carry out the 3D segmentation. It is a purely data driven method which is generic but has shown to be robust towards weak edge and image noise interference, and has the ability to cope with difficult initialisations, such as cross boundary initialisation and converging to narrow and long passages which is common in vascular structures. To cope with the size of the dataset, we use an efficient implementation to speed up the segmentation.

Let the 3D grey level image be described by function $I(\mathbf{x})$ where $\mathbf{x} = [x,y,z]^T \in \mathscr{D}$ is a point in the image domain $\mathscr{D}$. Let Ω be an object to be segmented. We employ the level set method in which the object boundary $\partial\Omega(t)$ is defined through level set function $\Phi(\mathbf{x},t)$: $\partial\Omega(t) = \{\mathbf{x} : \Phi(\mathbf{x},t) = 0\}$. The most commonly used PDE to compute $\Phi(\mathbf{x},t)$ can be formulated as:

$$\frac{\partial\Phi}{\partial t} = \alpha\, g(\mathbf{x})\, \kappa(\mathbf{x},t)\, \|\nabla\Phi\| - (1-\alpha)(\mathbf{F}(\mathbf{x})\cdot\nabla\Phi) \tag{1}$$

where α is a real constant, $g(\mathbf{x}) = 1/(1+\|\nabla I\|)$ is the edge stopping function, $\kappa(\mathbf{x},t) = \nabla\cdot\hat{\mathbf{n}}$ is the mean curvature of surface $\Phi = const$, $\hat{\mathbf{n}} = \nabla\Phi/\|\nabla\Phi\|$ is the unit normal vector to that surface, $\mathbf{F}(\mathbf{x}) = [F_x, F_y, F_z]^T$ is the flow function determined by image I. The geometrical potential force (GPF) proposed in [12] is computed as:

$$\mathbf{F}(\mathbf{x}) = G(\mathbf{x})\cdot\hat{\mathbf{n}}, \qquad G(\mathbf{x}) = P.V.\int_{\mathbf{x}'\in\mathscr{D}} \nabla I(\mathbf{x}')\cdot\frac{\mathbf{x}-\mathbf{x}'}{\|\mathbf{x}-\mathbf{x}'\|^{n+1}}\,\mathrm{d}^n\mathbf{x}', \tag{2}$$

where G is the scalar potential and $P.V.$ denotes the principle value (as the integral can diverge in vicinity $\mathbf{x}' = \mathbf{x}$), and $n = 3$ is the image dimension. This potential can be also represented as a convolution operation: $G = \nabla I * \mathbf{K}$ where $\mathbf{K} = P.V.\left(\mathbf{x}/\|\mathbf{x}\|^{n+1}\right)$ is the vector kernel (note that the convolution is united with the dot-product as ∇I and $\mathbf{K}$ are vectors). A discrete

analogue of the convolution kernel is $\mathbf{K}(\mathbf{x}) = \mathbf{x}/\|\mathbf{x}\|^{n+1}$ if $\mathbf{x} \neq \mathbf{0}$ and $\mathbf{0}$ if $\mathbf{x} = \mathbf{0}$. An efficient way to implement the convolution (2) is to apply the Fast Fourier Transform (FFT) method.

Equation (1) is solved numerically by using the finite difference method: using upwind scheme for the flow $\mathbf{F} \cdot \nabla\Phi$ and central differences for other derivatives. Advancing in time is performed by the forward Euler method. It is possible to show that in the 2D case with $n = 2$ this force coincides with a magnetic-active force [11]. Compared with the other image gradient based segmentation methods, this method is more stable to topological complexity of the object, to image noise, to model initialisation, to leakaged at fuzzy edges as shown in [12].

Improvements to the GPF method. When applied to 3D and large dataset it requires substantial amount of memory and computation still can be demanding even using FFT, as it is necessary to store arrays for all components of ∇I, for all components of kernel $\mathbf{K}$, and twice more for the results of the FFT evaluation. This drawback was an essential restriction of the method proposed in [12] if applied to the typical size of 3D medical scans.

To alleviate this, we re-write the integrand in (2) so that the integral is represented as convolution of scalar functions. Let $\tilde{I}(\mathbf{k})$ denote the Fourier transform of the image $I(\mathbf{x})$:

$$\tilde{I}(\mathbf{k}) = \int I(\mathbf{x}) e^{i\mathbf{k}\mathbf{x}} \mathrm{d}^n\mathbf{x} \tag{3}$$

where $\mathbf{k} = [k_x, k_y, k_z]^T$ (if $n = 3$). Then $\tilde{\nabla} I = i\mathbf{k}\tilde{I}$ and $\tilde{G} = (i\mathbf{k}\tilde{I}) \cdot \tilde{\mathbf{K}}^*$. The last equation can be re-written as

$$\tilde{G} = \tilde{I}(-i\mathbf{k} \cdot \tilde{\mathbf{K}})^* \qquad \Longleftrightarrow \qquad G = -I * (\operatorname{div} \mathbf{K}) \tag{4}$$

Scalar kernel $K = (\operatorname{div} \mathbf{K})$ behaves as $\|\mathbf{x}\|^{-(n+1)}$ when $\mathbf{x} \neq \mathbf{0}$ and has a strong singularity at $\mathbf{x} \neq \mathbf{0}$ such that $\int K(\mathbf{x})\, \mathrm{d}^n\mathbf{x} = 0$. In virtue of these properties, the discrete analogue is

$$K(\mathbf{x}) = \begin{cases} \|\mathbf{x}\|^{-(n+1)}, & \mathbf{x} \neq \mathbf{0} \\ -S, & \mathbf{x} = \mathbf{0} \end{cases}, \qquad S = \sum_{\mathbf{x} \in \Omega, \mathbf{x} \neq \mathbf{0}} \|\mathbf{x}\|^{-(n+1)}. \tag{5}$$

The potential G is a linear transform of I. It can be precomputed before evolving the deformable model (2). An example of 3D segmentation using this method is shown in Figure 1. It producd visually the same result as the original GPF method but it is more efficient and uses three times less memory.

3 Mesh generation

Despite a significant effort in developing robust patient-specific meshing methods, generation of a valid mesh automatically and rapidly is a challenge. A valid mesh for cardiovascular flows should be sufficiently fine to capture WSS with minimal error associated with point distribution. Using a coarse and purely unstructured mesh can produce a WSS distribution that is far from a converged solution. Although mesh convergence is not always straightforward to carry out, designing a mesh by taking into account all the necessary factors, including boundary layer, is essential to obtain results with high level of accuracy.

In patient-specific modelling, it is essential to have smooth transfer of image segmentation results to the meshing stage. In the majority of works reported, this link is often not well defined. Patient-specific meshing is a growing area of research, and currently, there is no universal way of satisfying all the meshing requirements via a single algorithm. In particulalr,

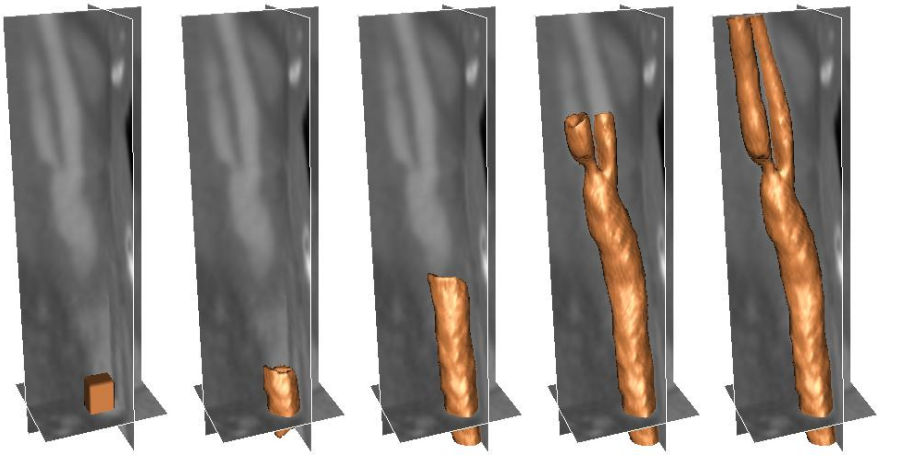

Figure 1: Segmentation of carotid artery from CT scan using the GPF deformable model with improved efficiency.

the interface between image processing and a valid surface generationis not satisfactorily addressed.

In standard engineering applications, the object boundary is rigorously defined and described analytically or piecewise analytically. A well-defined boundary allows to simplify the construction of a surface mesh and the corresponding cosmetics. In patient-specific medical objects, the surface is not well-defined and it may not be easily described analytically or piecewise analytically without compromising important surface features. Hence, alternative approaches have to be used and often it is essential to approximate the surface of a medical object. In this work, we generate surface meshes using the converged level set function from the segmentation, followed by boundary layer meshing.

The segmented domain is to be discretised, i.e. to build a conformal mesh of polyhedron elements approximating the domain as accurate as possible. We use a tetrahedron mesh with triangular surface elements in our simulation. The performance of a solution scheme depends significantly on the mesh quality. The elements should be of appropriate size, quality and shape to obtain a sensible and accurate numerical solution. The meshing stage also includes the accurate determination of the object inlet and outlets which should be orthogonal to the blood-vessel.

Surface meshing. The surface mesh generation procedure has the following stages.

1) The level set function calculated by the segmentation is used to determine the approximate axis of the arteries and their branches. These skeleton-like structures are useful in automatic identification of the geometrical features of the vessel, such as stenosis, aneurysms, bifurcations and kinks. It is also helpful for determining the appropriate orientations for the inlet and outlet surfaces. We apply voxel thinning algorithm to perform the skeletonisation, followed by axis smoothing to remove minor irregularities from skeletonisation.

2) Representation of the object surface through a continuous level set function gives an opportunity to employ an advanced Marching Cube (MC) algorithm [2] to obtain the surface. This gives a much smoother surface than the standard MC method.

3) Once a satisfactory surface representation is established and the geometrical skeleton

is generated, we are then bale to obtain the valid inlet and exit boundary surfaces. Often clipping is carried out manually, but in this work, we perform this automatically by using the generated surface and skeletons.

4) The mesh obtained by the advanced MC method often contains a large number of ill-shaped elements. In addition, the triangular element size can be smaller or larger than the element size required by the flow solver. Therefore, the initial mesh needs some further refinement, which creates a surface mesh for the same domain with much better element quality and at a prescribed element size. Here, we apply three procedures to improve the mesh quality:

(i) Mesh smoothing (no topological changes). We use the Taubin smoothing instead of traditional Laplace smoothing which can cause undesired shrinking of the objects.

(ii) Edge swapping. Topology based edge swapping is employed. The edge is swapped if the nodal index (number of contiguous modes) of vertices of triangles containing given edge becomes closer to an ideal value that is 6.

(iii) Splitting/contraction of edges. A too long edge is split by inserting a new node on a surface near the midpoint of the edge. A too short edge is reduced to a point on a surface near the midpoint of the contracted edge. Following the splitting and contraction the local mesh cosmetics is applied.

Volume meshing. To resolve the viscous boundary layer in flow studies, a special structure of the near-wall volumetric mesh is required. The elements built in the direction of inward normal to the wall should be essentially smaller than the element size in the inner volume of an artery. The short edge of a near-boundary tetrahedra should be directed normal to the wall. Such a quasi-structured, near-boundary mesh consists of N sub-layers with decreasing thickness towards the boundary. The mesh can be generated if we build triangular prisms at every face, by dividing every prism into N smaller prisms with height ratio f between two neighbouring prisms. To obtain a tetrahedron mesh, every triangular prism can be split into three tetrahedra. In [1], it is shown that $N = 10$ sub-layers is sufficient to evaluate WSS with the desired accuracy. Additional 3D smoothing technique based on 3D Lloyd's [3] iterations is also applied. Figure 2 gives an example of the meshing process and it also shows the computed WSS distribution.

4 Flow solution

The waveform of the inlet maximal velocity is extracted from ultrasound measurements [4], and the boundary conditions in the inlet are computed as a generalisation of the Womersley solution [9] onto non-circular pipe [7]. The boundary condition in the inlet is specified such that the mass flow through the considered part of the blood vessel is appropriate and the outlets have a realistic split of the mass flow at the branches. The vessel wall a considered a rigid in this study. In order to model biofluid flows, the locally conservative Galerkin (LCG) method is employed within the characteristic based split (CBS) scheme [5]. To account for possible turbulence, a Sparlart-Allmaras (SA) turbulence model is employed [8]. The influence of the boundary mesh parameters on convergence of the solution have been investigated. From the CFD simulation, information on the flow patterns, pressure distribution, and wall shear stress (WSS) has been determined, together with further WSS derived parameters which have been linked to intima-media thickness and risk of atheroma.

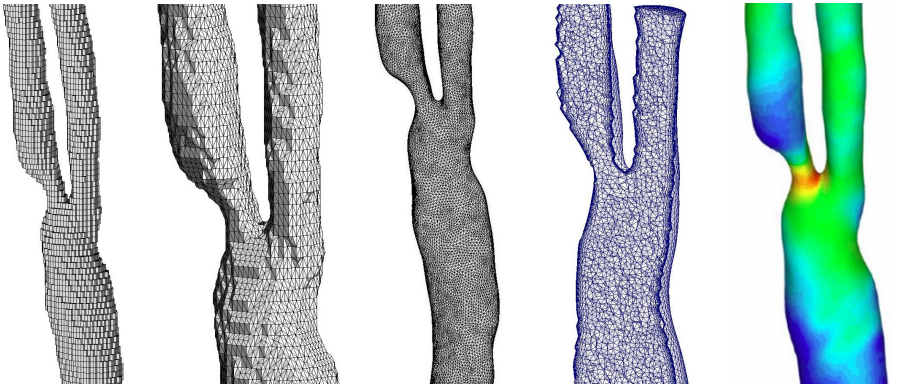

Figure 2: Meshing stages: (a) binary image, (b) initial mesh, (c) surface mesh after cosmetics, (d) a cut off view of the volumetric mesh. (e): time-averaged WSS distribution.

5 Conclusion

In this paper, we briefly presented a pipeline for patient-specific computational modelling from medical image scan, to segmentation, to mesh generation and finally to computational simulation. The focus of this work is on segmentation, which is based on an extension of the GPF model, and computational mesh generation. Automatic mesh generation is particularly difficult due to the complexity of the structure and high mesh quality demand from finite element based simulation. The proposed method showed promising results towards a fully automated segmentation and meshing process.

References

[1] R.L.T. Bevan, P. Nithiarasu, R. Van Loon, I. Sazonov, H. Luckraz, and A. Garnham. Application of a locally conservative Galerkin (LCG) method for modelling blood flow through a patient-specific carotid bifurcation. 64:1274–1295, 2010.

[2] E. V. Chernyaev. Marching cubes 33: Construction of topologically correct isosurfaces. Technical report Cern CN 95-17, CERN, 1995.

[3] Q. Du and D. Wang. Tetrahedral mesh generation and optimization based on CVT. *International Journal for Numerical Methods in Engineering*, 56:1355–1375, 2003.

[4] D.W. Holdsworth, C.J.D. Norley, R Frayne, DA Steinman, and BK Rutt. Characterization of common carotid artery blood-flow waveforms in normal human subjects. *Physiological Measurement*, 20(3):219–240, 1999.

[5] C.B. Liu and P. Nithiarasu. The explicit characteristic based split (cbs) method for viscoelastic flow past a circular cylinder. *International Journal for Numerical Methods in Fluids*, 57:157–176, 2008.

[6] R. Malladi, J. A. Sethian, and B. C. Vemuri. Shape modelling with front propagation: A level set approach. *IEEE T-PAMI*, 17(2):158–175, 1995.

[7] I. Sazonov, S.-Y. Yeo, R. L. T. Bevan, X. Xie, R. van Loon, and P. Nithiarasu. Modelling pipeline for subject-specific arterial blood flow -A review. *International Journal for Numerical Methods in Biomedical Engineering*, 27(8):1167–1184, 2011.

[8] P.R. Spalart and S.R. Allmaras. A one-equation turbulence model for aerodynamic flows. *AIAA paper 92-0439*, 1992.

[9] J.R. Womersley. Oscillatory flow in arteries: the constrained elastic tube as a model of arterial flow and pulse transmission. *Physics in Medicine and Biology*, 2:178–187, 1957.

[10] X. Xie. Active contouring based on gradient vector interaction and constrained level set diffusion. *IEEE T-IP*, 19(1):154–164, 2010.

[11] X. Xie and M. Mirmehdi. MAC: Magnetostatic active contour model. *IEEE T-PAMI*, 30(4): 632–647, 2008.

[12] S. Y. Yeo, X. Xie, I. Sazonov, and P. Nithiarasu. Geometrically induced force interaction for three-dimensional deformable models. *IEEE T-IP*, 20(5):1373–1387, 2011.